きたところである。薬剤のない時代には選択の余地がなく，副作用などと戦いながら治療してきたが，現在では適正な使用が求められる時代に入っており，正しい知識の習得が求められる。

文　　献

1) 深在性真菌症のガイドライン作成委員会編：深在性真菌症の診断・治療ガイドライン．協和企画，東京，2007.
2) B. D. Pauw, T. J. Walsh, J. P. Donnelly, et al.: Revised definitions of invasive fungal disease from the European Organization for Research and Treatment of Cancer/Invasive Fungal Infections Cooperative Group and the National Institute of Allergy and Infectious Diseases Mycoses Study Group (EORTC/MSG) Consensus Group. Clin Infect Dis, 46(12): 1813-1821, Jun 15, 2008.
3) Ansorg, R., van den Boom, R., Rath, P. M.: Detection of Aspergillus galactmannan antigen in foods and antimicrotics. Mycoses, 40: p353-357, 1997.
4) Pappas, P. G., Kauffman, C. A., Andes, D., Benjamin, D. K. Jr., Calandra, T. F., Edwards, J. E. Jr., Filler, S. G., Fisher, J. F., Kullberg, B. J., Ostrosky-Zeichner, L., Reboli, A. C., Rex, J. H., Walsh, T. J., Sobel, J. D.: Infectious Diseases Society of America. Clinical practice guidelines for the management of candidiasis: 2009 update by the Infectious Diseases Society of America. Clin Infect Dis, 48(5): 503-535, Mar 1, 2009.
5) Andes, D.: Antifungal pharmacokinetics and pharmacodynamics: understanding the implications for antifungal drug resistance. Drug Resist Updat, 7: 185-194, 2004.

Endocrine Journal 2009, **56** (8), 919-920

EDITORIAL

Molecular Targeted Therapy for Thyroid Cancer in Japan: A Call to Reduce the Backlog

SHUNICHI YAMASHITA

Professor of Molecular Medicine,
Dean, Graduate School of Biomedical Sciences,
Nagasaki University

Background

Thyroid cancer is the most common endocrine malignancy. Differentiated thyroid cancers, such as papillary and follicular thyroid carcinomas (PTC and FTC, respectively), are often curable with surgical resection in conjunction with hormone suppression therapy and radioactive iodine. However, a small number of patients do not achieve remission and need further or new therapeutic interventions. Recent molecular investigations have elucidated the complex genetic mechanisms of thyroid cancer, demonstrating the involvement of multiple signal transduction pathways and thus making the targeting of specific molecules possible.

The RAS-RAF-MEK-ERK signaling cascade (the so-called MAP kinase pathway) is pivotal for both PTC and FTC. In PTC, the activating mutations in the gene encoding a serine/threonine kinase BRAF and gene rearrangements involving *RET* (*RET/PTC* rearrangements) result in the constitutive activation of the pathway which occurs in the majority of cases (50–70%) in most populations in the world. Similarly, the activating mutations in the *RAS* family protooncogenes are found in 15–30% of FTCs. The available data suggest that *BRAF* mutation is associated with a more aggressive phenotype and radioiodine-refractory behavior.

Aims for Molecular Targeted Therapy

The inhibition of intracellular signaling by newly developed compounds that directly or indirectly block protein kinase activity of some upstream or downstream factors in the RAS-RAF-MEK-ERK and PI3K-PDK1-AKT-mTOR cascades induces thyroid cancer cell death *in vitro* and *in vivo*. In addition, the overexpression and/or hyperfunctioning of vascular endothelial growth factor (VEGF) and its receptors, hepatocyte growth factor (HGF) and its receptor (MET), and platelet derived growth factor (PDGF) and its corresponding receptors are well-described in thyroid cancer. Therefore, multiplex kinase inhibitors capable of disrupting these pathways are the first-line candidates for molecular targeted therapy for refractory tumors. Agents restoring radioiodine uptake such as histone deacetylase (HDAC) inhibitors and retinoid derivatives represent another promising field in new drug development. We have also reported the effectiveness of Gleevec for progressive thyroid cancer both *in vitro* and *in vivo* by inhibiting elevated c-ABL kinase activity which is closely linked with aberrant p53. Hence, the restoration and/or normalization of p53 function is a critical molecule-targeting task in advanced thyroid cancers such as anaplastic carcinoma. The selective inhibitor(s) of NF-κB is also a good candidate for advanced thyroid cancer therapy. In a longer-range outlook, the expanding knowledge of the role of cancer stem cells in human malignancies is another exciting idea particularly important in the context of molecular targeted therapy. Provided it is explored in greater detail and holds true for thyroid cancer, a major breakthrough in pharmacological approaches to the treatment of life-threatening forms of thyroid cancer could well be expected.

Realization of Clinical Trials

Taken together with the rapid progress in the development and preclinical testing of molecule-targeting agents for advanced thyroid cancers, real clinical trials, now in Phase II and III, have been initiated in the USA and Europe on the basis of a well-established multicenter international research consortium under the oversight of an ethical committee that attended to legal issues and ensured the protection of patient safety. Unfortunately, Japan is far behind this impor-

tant world trend, partly because of its poor registration system and its lack of a control tower of clinical trials at the level of neutral research centers devoid of conflict of interest. Without any control of clinical trials in general, it is difficult to make a convincing case for the reconsideration of conventional treatment and the application of the effectiveness of known chemotherapy combinations for rare but crucial cases of advanced thyroid cancers. Furthermore, the Pharmaceutical Affairs Act promulgated by the Japanese Ministry of Health, Welfare, and Labor may neither be well matched with the laws of other western countries nor capable of acting swiftly enough to the rapid global competition in medical applications from the standpoint of risk and benefit for the patients.

Although clinical trials in Japan are currently promoted within the framework of the Japan Clinical Oncology Group (JCOG) aimed at various solid cancers, the Japanese Endocrine Society as well as the Japan Thyroid Association has so far not established any close working relationship with the JCOG. The shortage of endocrine oncologists is also another major problem.

Conclusions

To overcome these handicaps and to bring us to the forefront of clinical trials of molecular targeted therapies especially for advanced and poor-prognosis thyroid cancers, it is urgently necessary for us to form a strong comprehensive mechanism of translational research and also to establish a strategic hospital-based network that would integrate pharmaceutical companies and manage patient participation in collaboration with the JCOG as well as with the American Thyroid Association and the European Thyroid Association. Such efforts would definitely improve the standards of thyroid cancer treatment through the testing of new therapeutic regimens or combined modalities much more objectively, efficiently, and safely.

Endocrine Journal 2009, **56** (2), 257–261

Urinary Iodine Concentrations in Urban and Rural Areas around Chernobyl Nuclear Power Plant

YASUYUKI TAIRA*,***, NAOMI HAYASHIDA*, SERGEY ZHAVARANAK#, ALEXANDER KOZLOVSKY##, ANATOLY LYZIKOV##, SHUNICHI YAMASHITA** AND NOBORU TAKAMURA*

**Department of Radiation Epidemiology, Nagasaki University Graduate School of Biomedical Sciences, Nagasaki, Japan*
***Department of Molecular Medicine, Nagasaki University Graduate School of Biomedical Sciences, Nagasaki, Japan*
****Nagasaki Prefectural Institute for Environmental Research and Public Health, Nagasaki, Japan*
#Belarussian Medical Academy for Postgraduate Education, Minsk, Belarus
##Gomel State Medical University, Gomel, Belarus

Abstract. In 2007, we screened urinary iodine (UI) concentrations in urban (Gomel city) and in rural areas (Hoiniki city) of the Gomel Region, Republic of Belarus, which was heavily contaminated by the accident at the Chernobyl Nuclear Power Plant, in order to evaluate the current state of iodine supplementation in these areas. Median levels of UI were 220.5 μg/L (151.5–358.5) μg/L in Gomel city, and 228.0 μg/L (130.0–337.5) μg/L in Hoiniki city. Urinary concentrations in Gomel city were significantly improved, as compared to our previous results in 2000 ($p<0.001$). There were no differences of UI concentrations between Gomel city and Hoiniki city ($p = 0.39$), and none of the samples showed moderate (<50 μg/L) or severe (<20 μg/L) iodine deficiency in either city. These results suggest that the state of iodine supplementation has improved in rural areas, as well as in urban areas in the Republic of Belarus, probably due to appropriate fortification of iodized salt in this region.

Key words: Urinary iodine, Chernobyl Nuclear Power Plant, Iodized salt, Iodine deficiency

(*Endocrine Journal* **56**: 257–261, 2009)

TWENTY-TWO years have passed since the Chernobyl accident, the worst nuclear accident in history. Medical examinations aimed at children performed within the framework of the International Programme on the Health Effects of the Chernobyl Accident (IPEHCA) and the Chernobyl Sasakawa Health and Medical Cooperative Project have shown a significant increase in the incidence of childhood thyroid cancer [1, 2]. In particular, in the Gomel region of the Republic of Belarus, a dramatic increase of thyroid cancer had been observed. In 2006, the World Health Organization (WHO) reported that the overall number of thyroid cancer cases diagnosed in Belarus, Ukraine and in the four most contaminated regions of Russia during 1986–2002 is above 4,000 among children and adolescents [3]. Over 2,000 cases were reported in Belarus alone.

One of the major components of the radionuclides released by the accident was iodine-131 (^{131}I). Radioactive iodine fallout led to considerable exposure in the population residing around the Power Plant through inhalation and ingestion of contaminated foodstuffs [3], which may have induced the increase in thyroid cancer after the accident. In a thyroid screening study, Shibata *et al.* compared the incidence of thyroid cancer in children born before April 26, 1986, during 1986, and after 1986 and found that that none of children born after 1986 had thyroid cancer, which strongly suggests that internal radiation exposure by short-lived radionuclides, such as ^{131}I contributed the increased incidence of thyroid cancer after the accident [4].

Received: September 16, 2008
Accepted: December 8, 2008
Correspondence to: Noboru TAKAMURA, M.D., Ph.D., Professor, Department of Radiation Epidemiology Nagasaki University Graduate School of Biomedical Sciences 1-12-4 Sakamoto, Nagasaki 852-8523, Japan

Experimental studies have shown that iodine deficiency may be an important modifier for the risk of radiation-induced thyroid cancer [5–7]. Iodine deficiency affects both the dose received by the thyroid gland at the moment of exposure, and if maintained, can affect thyroid function in the time after exposure [2, 8, 9]. Previous reports have shown that endemic goiter is relatively common in areas of Ukraine and Belarus due to iodine deficiency [10]. Ashizawa *et al.* screened urinary iodine (UI) concentrations around Chernobyl between 1991 and 1996, and confirmed an endemic iodine-deficient zone within this area [11]. Ishigaki *et al.* screened UI concentrations in the Gomel region in 2000, and showed that median UI concentration was 47.3 μg/L [12]. Tronko *et al.* also evaluated urinary iodine (UI) concentrations in subjects who participated in the Ukranian-American Cohort Study, and reported median UI concentrations of 41.7 μg/L for 1998–2000 and 47.5 μg/L for 2001–2003 [13], concluding that UI levels remained at mild-moderate deficiency levels in this area.

In 2005, we screened UI concentrations in Kiev, Ukraine, and showed that median UI concentration was 109 μg/L, and only 10 of 100 subjects (10%) showed moderate iodine deficiency (<50 μg/L), with none showing severe iodine deficiency (<20 μg/L), which suggested that iodine status in Ukraine is improving, probably due to supplementation with iodized salt [14]. We also screened UI concentrations in Semipalatinsk, Republic of Kazakhstan, and found no clear evidence of iodine deficiency in this area [15, 16], which suggests that socio-medical prophylaxis against iodine deficiency has been successfully implemented in the former USSR, mainly due to iodized salt.

In this study, we screened UI concentrations in urban (Gomel city) and in rural areas (Hoiniki city) of the Gomel Region, Republic of Belarus, in order to evaluate the current state of iodine supplementation in urban and rural areas of this country.

Materials and Methods

Subjects and Samples

Prior to this study, ethical approval was obtained from the special committee of Nagasaki University (project registration number: 14032639). After obtaining informed consent, we collected morning spot urine samples in Gomel city (n = 100; total population number: 481,000 in 2005), capital of the Gomel Region, and in Hoiniki city (n = 126; total population number: 17,000 in 2005), a rural town in the same Region. The location of each city is shown in Fig. 1 All samples were kept at 4°C until assay.

Fig. 1. Location of Gomel city and Hoiniki city in the Republic of Belarus.

Measurement of urinary iodine

UI concentration was measured by the "simple microplate method", based on the Sandell-Kolthoff reaction [17], incorporating both the reaction and digestion processes in microplate format, as described elsewhere [18]. Briefly, using a specially designed sealing cassette to prevent the loss of vapor and cross-contamination among plates, ammonium persulfate digestion was performed in a 96-well microtiter plate (MicroWell; Nalge Nunc International) in an oven at 110°C for 60 min. After digestion, the mixture was transferred to a transparent microplate and the Sandell-Kolthoff reaction was performed at 25°C for 30 min. Finally, UI concentration in each well was measured by microplate reader at 405 nm. The sensitivity of this method is >10 μg/L.

Statistical Analysis

UI concentrations were expressed as "medians (25^{th}–75^{th} percentiles)". According to the criteria of WHO, we defined mild iodine deficiency as 50–99 μg/L, moderate iodine deficiency as 20–49 μg/L, and severe iodine deficiency as less than 20 μg/L [19].

The results obtained at Gomel city were compared with previous results obtained in 2000 (n = 100) [12]. Differences in UI concentrations were evaluated by Mann-Whitney's U-test. Probability values of less than 0.05 were considered indicative of statistical significance. All statistical analyses were performed using SPSS v16.0 software (SPSS Japan, Tokyo, Japan).

Results and Discussion

UI concentration was 220.5 μg/L (151.0–358.8) in Gomel city, and was 228.0 μg/L (130.0–337.5) in Hoiniki city, respectively (Fig. 2). There were no significant differences in UI concentration between the two cities (p = 0.39). In Gomel city, UI concentrations were significantly improved when compared to our previous results in 2000 (220.5 μg/L (151.0–358.8) vs. 47.3 μg/L (35.9–76.5), p<0.001, Fig. 3). In 2000, 34% showed mild deficiency, 42% showed moderate deficiency and 10% showed severe deficiency in Gomel city (Table 1); whereas in 2007, only 7% of subjects showed mild UI deficiency (<100 μg/L) in Gomel city, and 11% showed mild UI deficiency in Hoiniki city. However, no one showed moderate and/or severe deficiency in either city.

The present results suggest that the state of iodine supplementation has markedly improved in Gomel city since 2000. Furthermore, we showed that there were no differences in UI concentration between urban and rural areas of the Gomel region, which suggests that iodine supplementation has successfully been implemented in both rural and urban areas. To our knowledge, this is the first report to show that both urban and rural areas of the Gomel region, Republic of Belarus, are no longer iodine deficient. During the current survey, we visited a local market and confirmed that all commercially distributed salts were iodized, which suggests that the improvement of iodine supplementation status in this area is due to appropriate fortification of iodized salt.

Recently, Cardis *et al.* analyzed the interaction between radiation dose and iodine deficiency on the risk of thyroid cancer in Belarus and Russia, and confirmed a significant interaction between dose, iodine levels in soil and risk of thyroid cancer [20]. Shakhtarin *et al.* also performed a similar study in the Bryansk region, Russia, and found a joint effect of radiation dose and iodine deficiency [21]. These results suggest that supplementation with iodine in deficient areas is needed in order to reduce the possible future risk of radiation-induced thyroid cancer around Chernobyl, as well as to reduce the risk of thyroid diseases, such as endemic goiter and congenital hypothyroidism.

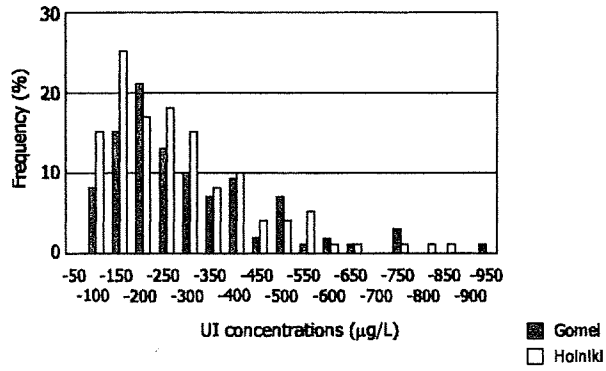

Fig. 2. Distribution of UI concentrations between Gomel city and Hoiniki city.

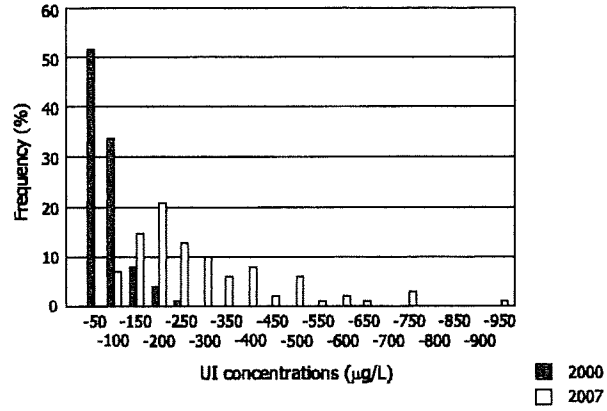

Fig. 3. Distribution of UI concentrations of Gomel city in 2000 and 2007.

In Belarus, early studies showed that the prevalence of endemic goiter due to iodine deficiency was mild to moderate [10]. A considerable decrease in the prevalence of endemic goiter was achieved between 1970 and 1980, but an overall rise was seen before 1990. As locally produced foodstuffs and water in Belarus had low iodine contents [10], this rise was probably due to political changes in the former USSR and Republic of Belarus, and the resulting lack of iodine supplementation in salt. Since 1999, large amounts of iodized salt have been supplied in Belarussian market [22]. However, there were still marked gap of iodized salt distribution between urban and rural areas of Belarus.

Table 1. Summary of UI concentration of each region and the number of cases (%) with iodine deficiencies

	Median UIconcentration (μg/L)	50–99 μg/L (mild deficiency)	20–49 μg/L (moderate deficiency)	<20 μg/L (severe deficiency)
Gomel (2000)	47.3	34/100 (34%)	42/100 (42%)	10/100 (10%)
Gomel (2007)	220.5	7/100 (7%)	—	—
Hoiniki (2007)	228.0	14/126 (11%)	—	—

Actually in 2003, households using adequate iodized salt were 83% in Minsk (capital of Belarus), whereas those in Gomel region (including Gomel and Hoiniki cities) region were 51% [23]. In this study, we demonstrated that iodine is now appropriately supplemented in rural and urban areas of the Gomel region. This suggests that iodine supplementation in salt is effective in rural areas, as well as urban areas of Belarus. As a high incidence of thyroid cancer had been observed in rural areas of Belarus, particularly in Hoiniki city in the Gomel region [24], careful follow up of iodine supplementation status, as well as of thyroid cancer incidence, is needed.

There are several limitations in the current study. We were able to collect urine samples only in Gomel and Hoiniki cities. Further collection is needed in other rural cities of the Gomel region, and in other contaminated areas. In addition, we did not perform morphological or immunological screening of thyroid glands in this area. Previously, we screened the prevalence of positive antimicrosomal antibodies and antithyroglobulin antibodies by sex and age at the time of examination in children aged 0–10 years at the time of the Chernobyl Nuclear Power Plant accident and examined at Gomel region in 1991–1996 [25]. Recently, Agate *et al.* also screened for the prevalence of antithyroglobulin and antithyroperoxidase antibodies in 1999–2001, and showed that the prevalence of antithyroperoxidase antibodies in adolescents exposed to radioactive fallout remained elevated in Belarus at 13–15 years after the accident, without thyroid dysfunction [26]. These suggest that radioactive fallout may elicit a transient autoimmune reaction, without triggering full-blown thyroid autoimmune disease. Long-term and systematic follow up is needed in addition to the evaluation of iodine supplementation.

In conclusion, we screened UI concentrations and showed that the state of iodine supplementation has improved in rural areas, as well as in urban areas, in the Republic of Belarus, probably due to appropriate fortification of iodized salt. Regular screening of thyroid status, including UI concentrations, particularly in young adults who were children at the time of the Chernobyl Nuclear Power Plant accident is required in order to control the radiation health risks in this area.

Acknowledgements

This work was supported by the Foundation for Growth Science and the Ministry of Education, Culture, Sports, Science and Technology of Japan through the Nagasaki University Global COE program. We would also like to thank Ms. Miho Yoshida for her technical assistance.

References

1. Souchkevitch GN, Tsyb AF (eds) (1997) Health consequences of the Chernobyl accident: results of the IPEHCA pilot projects and related national programmes. Geneva: WHO.
2. Yamashita S, Shibata Y (eds) (1997) Chernobyl a decade. ICS, 1156, Excerpta Medica, Amsterdam.
3. Bennet B, Repacholi M, Zhanat C (eds) (2006) Health Effects of the Chernobyl Accident and Special Health Care Programmes. Geneva: WHO.
4. Shibata Y, Yamashita S, Masyakin VB, Panasyuk GD, Nagataki S (2001) 15 years after Chernobyl: new evidence of thyroid cancer. *Lancet* 358: 1965–1966.
5. Thomas GA, Williams ED (1991) Reversibility of the malignant phenotype in monoclonal tumours in the mouse. *Br J Cancer* 63: 213–216.
6. Kanno J, Onodera H, Furuta K, Maekawa A, Kasuga T, Hayashi Y (1992) Tumour-promoting effects of both iodine deficiency and iodine excess in the rat thyroid. *Toxicol Pathol* 20: 226–235.
7. Ohshima M, Ward JM (1986) Dietary iodine deficien-

cy as a tumor promoter and carcinogen in male F344/NCr rats. Cancer Res 46: 877–883.
8. Baverstock K, Cardis E (1996) The WHO activities on thyroid cancer. Proceeding of the EU conference "The Radiological Consequences of the Chernobyl Accident".
9. Gemibicki M, Stozharov AN, Arinchin AN, Moschik KV, Petrenko S, Khamara IM, Baverstock KF (1997) Iodine deficiency in Belarusian children as a possible factor stimulating the irradiation of the thyroid gland during the Chernobyl catastrophe. *Environ Health Perspect* 89: 1779–1797.
10. Gerasimov G (1993) Update on IDD in the Former USSR. IDD Newsletter 9. http://www.iccidd.org/media/IDD%20Newsletter/1991–2006/idd1193.htm#USSR
11. Ashizawa K, Shibata Y, Yamashita S, Namba H, Hoshi M, Yokoyama N, Izumi M, Nagataki S (1997) Prevalence of goiter and urinary iodine excretion levels in children around Chernobyl. *J Clin Endocrinol Metab* 82: 3430–3433.
12. Ishigaki K, Namba H, Takamura N, Saiwai H, Parshin V, Ohashi T, Kanematsu T, Yamashita S (2001) Urinary iodine levels and thyroid diseases in children; comparison between Nagasaki and Chernobyl. *Endocr J* 48: 591–595.
13. Tronko M, Kravchenko V, Fink D, Hatch M, Turchin V, McConnell R, Shpak V, Brenner A, Robbins J, Lusanchuk I, Howe G (2005) Iodine excretion in regions of Ukraine affected by the Chernobyl accident: Experience of the Ukrainian-American cohort study of thyroid cancer and other thyroid diseases. *Thyroid* 15: 1291–1297.
14. Takamura N, Bebeshko V, Aoyagi K, Yamashita S, Saito H (2007) Ukraine urinary iodine levels; 20 years after the Chernobyl accident. *Endocr J* 54: 335.
15. Hamada A, Takamura N, Meirmanov S, Alipov G, Mine M, Ensebaev R, Sagandikova S, Ohashi T, Yamashita S (2003) No evidence of radiation risk for thyroid gland among schoolchildren around Semipalatinsk Nuclear Testing Site. *Endocr J* 50: 85–89.
16. Hamada A, Zakupbekova M, Sagandikova S, Espenbetova M, Ohashi T, Takamura N, Yamashita S (2003) Iodine prophylaxis around the Semipalatinsk Nuclear Testing Site, Republic of Kazakhstan. *Public Health Nutr* 6:785–789.
17. Sandel EB, Kplthoff IM (1937) Micro determination of iodine. *Microchem Acta* 1: 9–25.
18. Ohashi T, Yamaki M, Pandav CS, Karmarkar MG, Irie M (2000) Simple microplate method for determination of urinary iodine. *Clin Chem* 46: 529–536.
19. World Health Organization (2004) Iodine status worldwide. WHO global database on iodine deficiency. Geneva: World Health Organization.
20. Cardis E, Kesmeniene A, Ivanov V, Malakhova I, Shibata Y, Khrouch V (2005) Risk of thyroid cancer after exposure to ^{131}I in childhood. *J Natl Cancer Inst* 97: 724–732.
21. Shakhtarin VV, Tsyb AF, Stepanenko VF, Orlov MY, Kopecky KJ, Davis S (2003) Iodine deficiency, radiation dose, and the risk of thyroid cancer among children and adolescents in the Bryansk region of Russia following the Chernobyl power station accident. *Int J Epidemiol* 32: 584–591.
22. The United Nations Children's Fund (2002) The iodine deficiency elimination program in Belarus. The United Nations Children's Fund.
23. Gerasimov G (2003) The iodine deficiency elimination program in Belarus in 2003 End-of-the Year Review and Recommendations. The United Nations Children's Fund.
24. Yamashita S, Shibata Y, Hoshi M, Fujimura K (eds) (2002) Chernobyl: Message for the 21st Century. ICS, 1234, Excerpta Medica, Amsterdam.
25. Yamashita S, Shibata Y (eds) (1997) Chernobyl: A Decade. Elsevier Science.
26. Agate L, Mariotti S, Elisei R, Mossa P, Pacini F, Molinaro E, Grasso L, Masserini L, Mokhort T, Vorontsova T, Arynchyn A, Tronko MD, Tsyb A, Feldt-Rasmussen U, Juul A, Pinchera A (2008) Thyroid autoantibodies and thyroid function in subjects exposed to Chernobyl fallout during childhood: evidence for a transient radiation-induced elevation of serum thyroid antibodies without an increase in thyroid autoimmune disease. *J Clin Endocrinol Metab* 93: 2729–2736.

Endocrine Journal 2009, **56** (1), 161–164

NOTE

Mutation Analysis of RAP1 Gene in Papillary Thyroid Carcinomas

MICHIKO MATSUSE*, NORISATO MITSUTAKE*, TATIANA ROGOUNOVITCH*, VLADIMIR SAENKO**, YUKA NAKAZAWA*, PAVEL RUMYANTSEV***, EUGENY LUSHNIKOV#, KEIJI SUZUKI* AND SHUNICHI YAMASHITA*,**

**Department of Molecular Medicine, Atomic Bomb Disease Institute, Nagasaki University Graduate School of Biomedical Sciences, 1-12-4 Sakamoto, Nagasaki 852-8523, Japan*

***Department of International Health and Radiation Research, Atomic Bomb Disease Institute, Nagasaki University Graduate School of Biomedical Sciences, 1-12-4 Sakamoto, Nagasaki 852-8523, Japan*

****Department of Radiosurgery, Medical Radiological Research Center, 4 Korolev St., Obninsk 249036, Russia*

#Department of Pathology, Medical Radiological Research Center, 4 Korolev St., Obninsk 249036, Russia

Abstract. In human papillary thyroid carcinomas (PTCs), the genetic alterations of *RET/PTC, RAS* or *BRAF* account for about 60–70% of cases with practically no overlap, providing strong genetic evidence that constitutive active signaling along MAPK pathway is critical for PTC development. In the remaining 30–40% of the cases, the oncogenes are still unknown. RAP1 is a member of the RAS family of small G proteins transmitting signals from the TSH-R to MAPK pathway using cAMP-dependent mechanism in thyroid cells. RAP1 was shown to have both mitogenic and tumorigenic properties in certain systems; however, the potential role of *RAP1* mutation in thyroid carcinogenesis has yet to be elucidated. In this study, we analyzed the mutational status of *RAP1* gene in 36 Russian patients with PTCs without *RET/PTC* rearrangement, *BRAF* mutation or *RAS* mutation. No mutations in either *RAP1A* or *RAP1B* genes were found. These results suggest that *RAP1* mutation does not play an important role in PTC pathogenesis.

Key words: RAP1, Mutation, Papillary thyroid cancer

(*Endocrine Journal* **56**: 161–164, 2009)

PAPILLARY thyroid carcinoma (PTC) represents the most common malignant tumor in thyroid. PTCs have particular genetic alterations leading to the activation of the mitogen-activated protein kinase (MAPK) signaling pathway. Those alterations include *RET/PTC* rearrangement and point mutations in *BRAF* and *RAS* genes. They are detected in approximately 60–70% of all PTCs and rarely overlap in the same tumor [1–3]. The lack of concordance for these mutations provides strong genetic evidence for the requirement of constitutive activation of MAPK signaling for transformation to PTC. The remaining 30–40% of PTC cases do not have alterations in these genes, suggesting that other factors may contribute to constitutive activation of MAPK pathway.

There are three RAF isoforms in mammalian cells: ARAF, BRAF and CRAF (also known as RAF-1). CRAF is expressed ubiquitously, whereas ARAF and BRAF are expressed in a tissue-specific manner. Ras-associated protein-1 (RAP1) is a member of the RAS family of small G proteins and consists of two highly homologous isoforms, RAP1A and RAP1B. Although it was originally identified as an antagonist of RAS-induced transformation [4], subsequent studies have shown that RAP1 activation induces either inhibition or activation of MAPK cascade depending on type of cells [5]. RAP1 activation inhibits MAPK pathway by

Received: August 29, 2008
Accepted: October 12, 2008
Correspondence to: Norisato MITSUTAKE, M.D., Ph.D., Department of Molecular Medicine, Atomic Bomb Disease Institute, Nagasaki University Graduate School of Biomedical Sciences, 1-12-4 Sakamoto, Nagasaki 852-8523, Japan

blocking RAS binding to CRAF in BRAF-negative cells. By contrast, RAP1 activates BRAF and in turn MAPK cascade in BRAF-expressing cells [6, 7]. In thyroid cells, thyroid-stimulating hormone (TSH) stimulates MAPK signaling through cAMP-RAP1-BRAF [8], indicating that RAP1 is a MAPK activator in thyrocytes. Schematic signaling pathways are shown in Fig. 1.

Moreover, Ribeiro-Neto *et al.* demonstrated cAMP-dependent oncogenic role of RAP1 in mice thyroid gland using transgenic animal model [9]. Recently, it has also been shown that downregulation of RAP1GAP, a negative regulator of RAP1, contributes to the RAS-induced transformation of thyroid cells [10]. Indeed, RAP1GAP expression was reduced in cancer lesion compared to normal follicular cells in clinical PTC specimens [10]. These data suggest that *RAP1* might be a good candidate as a target of oncogenic mutation in PTCs. Although Vanvooren *et al.* investigated mutational status of *RAP1* in follicular thyroid adenomas and did not find any mutations [11], it remains to be clarified whether RAP1 is activated by somatic mutation in PTCs. In this study, therefore, the possibility that *RAP1* mutation plays a role in PTC pathogenesis was explored.

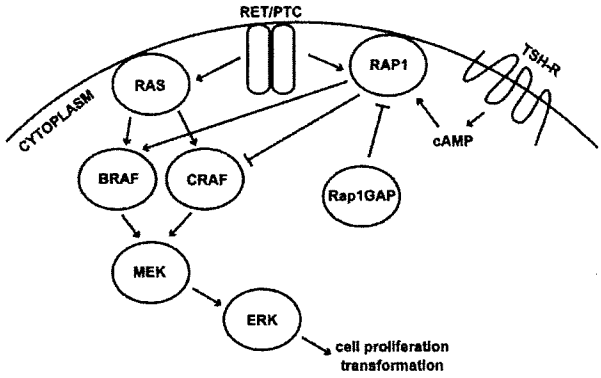

Fig. 1. Schematic oncogenic signaling pathways in PTC cells. In thyroid follicular cells, although RAP1 inhibits CRAF activation, TSH signal activates MAPK pathway through cAMP-RAP1-BRAF. Besides, all major oncoproteins such as RET/PTC, RAS or BRAF activate MAPK, and they rarely overlap in the same tumor, suggesting that the constitutive activation of the MAPK pathway is the key to PTC development.

Materials and Methods

PTC samples

All PTC patients were surgically treated at the Medical Radiological Research Center of Russian Academy of Medical Sciences (MRRC RAMS, Obninsk, Russian Federation) during 2000–2006; none of them had a history of radiation exposure. An appropriate informed consent was obtained from each individual according to ethical guidelines for the use of human materials for scientific purposes effective in MRRC RAMS. The present study is based on the agreement of academic cooperation between MRRC RAMS and Nagasaki University. Protocols for the present study were approved by the Committee for Ethical Issues of Human Genome Analysis of Nagasaki University. All samples were collected at the time of primary surgery and did not include recurrence. Forty-two frozen PTC samples from 36 patients (36 primary tumors and 6 metastatic lymph nodes, no multiple cancer) without *RET/PTC1*, *RET/PTC3*, $BRAF^{V600E}$ or *RAS* mutation were subjected to DNA (conventional proteinase K/phenol protocol) and RNA (using ISOGEN, Nippon Gene, Tokyo, Japan) extraction. Clinical and pathological characteristics of the patients are listed in Table 1.

Table 1. Clinical and pathological characteristics

	n = 36
Sex (female:male)	29 : 7
Age (years, mean ± SD)	44.89 ± 11.94
Tumor size (mm, mean ± SD)	19.09 ± 16.81 ([b]n = 32)
[a]Pathological TNM	[b]n = 32
T1	17 (53.1%)
T2	2 (6.3%)
T3	10 (31.3%)
T4a	2 (6.3%)
T4b	1 (3.1%)
N0	18 (56.3%)
N1a	4 (12.5%)
N1b	10 (31.3%)
M0	31 (96.9%)
M1	1 (3.1%)

[a] According to UICC/AJCC classification

[b] The records of four of the patients are not available.

Table 2. List of primers and PCR conditions

Gene	Primer	Primer sequence	Annealing temp (°C)	Amplicon size (bp)
RAP1A	RAP1A ex2 F	5'-CACATCATGCGTGAGTACAAGCTAGT-3'	57	604
	RAP1A ex7 R	5'-TTCATTCCTGTAATCTGGCTCAGAG-3'		
RAP1B	RAP1B F1 int2	5'-TTTTCTTCTACCTCTGAGCATCTTTTA-3'	56	2099
	RAP1B R1 int4	5'-GGTAACTATGCAATGCCAGAAAGT-3'		
	RAP1B int3 seq1 R	5'-AGAGAATATGATCCACCCAGATATAA-3'		
	RAP1B F2 int4	5'-TCCATATTGAGACTGGTTCGTGTAG-3'	56	2678
	RAP1B R2 int6	5'-TGTATGGGTATTTTTGCCTTTCA-3'		
	RAP1B int5 seq2 F2	5'-TACTACAGTATTCTTCATTGAGCTATAA-3'		
	RAP1B F3 int6	5'-CCTTTGGAGTTATCGTTTGCAT-3'	58	1591
	RAP1B R3 int8	5'-GGCAGATCACGAGGTCAAGAG-3'		

Sequence analysis

Amplification of RAP1B gene was performed by genomic PCR using Ex Taq HS (TaKaRa Bio, Ohtsu, Japan). For RAP1A, RT-PCR was done. Briefly, total RNA was reverse transcribed using MMLV-RT (Applied Biosystems, Foster City, CA, USA) and random hexamers to generate cDNA. Subsequent PCR amplification was done using ExTaq HS. The sequence of used primers, annealing temperature and amplicon size are listed in Table 2. The schema of the genes and primer locations are also shown in Fig. 2. PCR products were then treated with ExoSAP-IT (USB Corp., Cleveland, OH, USA), and sequence analysis was performed with a Big Dye Terminator sequencing kit version 3.1 (Applied Biosystems) and an ABI3100 automated sequencer (Applied Biosystems).

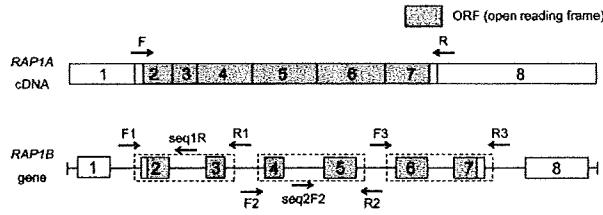

Fig. 2. Primers used for amplification and sequencing of *RAP1* genes. Exon numbers are indicated. For *RAP1A* analysis, we used the same primers for amplification and sequencing. Amplification of *RAP1B* gene was performed by genomic PCR using three primer sets: F1/R1, F2/R2 and F3/R3. For subsequent sequencing, we used seq1R primer for exon 2, R1 primer for exon 3, F2 primer for exon 4, seq2F2 primer for exon 5, F3 primer for exon 6 and R3 primer for exon 7. Shaded region indicates open reading frame (ORF), and sequences of entire ORF in both genes were analyzed (except a small part of the 5' end of *RAP1A*).

Results and Discussion

Since the mutations along the MAPK pathway in PTCs are virtually non-overlapping, a total of 42 PTC samples without *RET/PTC1*, *RET/PTC3*, $BRAF^{V600E}$ or hotspot mutations (codons 12, 13 and 61) in three *RAS* genes (*HRAS*, *KRAS* and *NRAS*) were available for this study. Specimens harboring the above alterations had been identified in preliminary screening resulting in 3.5% *RET/PTC*, 54.4% *BRAF* mutation and 3.4% *RAS* mutation (data not shown, technical details are available from the authors upon request), and were excluded from the *RAP1* analysis.

The samples with no known mutations were subjected to RT-PCR and direct sequencing for *RAP1A* analysis. Among those examined, no mutation was found in the coding region of *RAP1A* cDNA, except for the first 20 bases including translation start site (ATG). The analysis of the area was missed because these first 20 bases are included in the RAP1Aex2F primer sequence. Since we had difficulties in the PCR reaction with the primer located at 5' UTR, presumably due to GC rich area, we decided to use RAP1Aex2F. Note that RAP1 shares extensive homology with RAS [13], and no oncogenic mutation was found in the corresponding area in RAS. For RAP1B analysis, we performed three genomic PCRs to cover the coding region instead of RT-PCR, because there is a processed pseudogene called *hRAP1B-retro* on chromosome 5

[12]. The nucleotide sequence of coding region of *hRAP1-retro* differs only three positions from that of *RAP1B*, and we wanted to avoid the possibility of contamination. All primers for *RAP1B* analysis were located in intron regions. We analyzed 42 samples with wild-type *RAP1A*, and no mutation was identified in the coding region of the *RAP1B* gene. We also checked the status of known single nucleotide polymorphisms (SNPs) in both genes and found only major-allele (same as contig reference) signals at all locations.

To our knowledge, there has been only one paper reporting somatic *RAP1* mutation in human tumors. Gyan *et al.* found *RAP1B* mutation in one case out of 85 myelodysplastic syndromes (MDS) [13], but later Zemojtel *et al.* reported that the mutant *RAP1B* identified by Gyan *et al.* was not actually *RAP1B* gene but most likely *hRAP1B-retro* [12]. Thus, *RAP1* mutation does not seem to play a role in human carcinogenesis.

In conclusion, our data suggest that *RAP1* mutation does not appear to be a frequent target for oncogenic mutation in PTCs. However, its activation could potentially contribute to PTC carcinogenesis by other mechanisms such as overexpression of RAP1 or down-regulation of RAP1 inhibitor RAP1GAP.

Acknowledgements

This work was supported in part by Grant-in-Aid for Scientific Research (#19256003, #19390253, #19790651 and #20790662) and Global COE Program from the Ministry of Education, Culture, Sports, Science and Technology of Japan.

References

1. Kimura ET, Nikiforova MN, Zhu Z, Knauf JA, Nikiforov YE, Fagin JA (2003) High prevalence of BRAF mutations in thyroid cancer: genetic evidence for constitutive activation of the RET/PTC-RAS-BRAF signaling pathway in papillary thyroid carcinoma. *Cancer Res* 63: 1454–1457.
2. Soares P, Trovisco V, Rocha AS, Lima J, Castro P, Preto A, Maximo V, Botelho T, Seruca R, Sobrinho-Simoes M (2003) BRAF mutations and RET/PTC rearrangements are alternative events in the etiopathogenesis of PTC. *Oncogene* 22: 4578–4580.
3. Frattini M, Ferrario C, Bressan P, Balestra D, De Cecco L, Mondellini P, Bongarzone I, Collini P, Gariboldi M, Pilotti S, Pierotti MA, Greco A (2004) Alternative mutations of BRAF, RET and NTRK1 are associated with similar but distinct gene expression patterns in papillary thyroid cancer. *Oncogene* 23: 7436–7440.
4. Kitayama H, Sugimoto Y, Matsuzaki T, Ikawa Y, Noda M (1989) A ras-related gene with transformation suppressor activity. *Cell* 56: 77–84.
5. Stork PJ (2003) Does Rap1 deserve a bad Rap? *Trends Biochem Sci* 28: 267–275.
6. Vossler MR, Yao H, York RD, Pan MG, Rim CS, Stork PJ (1997) cAMP activates MAP kinase and Elk-1 through a B-Raf- and Rap1-dependent pathway. *Cell* 89: 73–82.
7. Stork PJ, Schmitt JM (2002) Crosstalk between cAMP and MAP kinase signaling in the regulation of cell proliferation. *Trends Cell Biol* 12: 258–266.
8. Iacovelli L, Capobianco L, Salvatore L, Sallese M, D'Ancona GM, De Blasi A (2001) Thyrotropin activates mitogen-activated protein kinase pathway in FRTL-5 by a cAMP-dependent protein kinase A-independent mechanism. *Mol Pharmacol* 60: 924–933.
9. Ribeiro-Neto F, Leon A, Urbani-Brocard J, Lou L, Nyska A, Altschuler DL (2004) cAMP-dependent oncogenic action of Rap1b in the thyroid gland. *J Biol Chem* 279: 46868–46875.
10. Tsygankova OM, Prendergast GV, Puttaswamy K, Wang Y, Feldman MD, Wang H, Brose MS, Meinkoth JL (2007) Downregulation of Rap1GAP contributes to Ras transformation. *Mol Cell Biol* 27: 6647–6658.
11. Vanvooren V, Allgeier A, Nguyen M, Massart C, Parma J, Dumont JE, Van Sande J (2001) Mutation analysis of the Epac—Rap1 signaling pathway in cold thyroid follicular adenomas. *Eur J Endocrinol* 144: 605–610.
12. Zemojtel T, Penzkofer T, Duchniewicz M, Zwartkruis FJ (2006) HRap1B-retro: a novel human processed rap1B gene blurs the picture? *Leukemia* 20: 145–146; author reply 146–147.
13. Gyan E, Frew M, Bowen D, Beldjord C, Preudhomme C, Lacombe C, Mayeux P, Dreyfus F, Porteu F, Fontenay M (2005) Mutation in RAP1 is a rare event in myelodysplastic syndromes. *Leukemia* 19: 1678–1680.

Published online 29 January 2009

Nucleic Acids Research, 2009, Vol. 37, No. 4 e31
doi:10.1093/nar/gkp023

A rapid non-radioactive technique for measurement of repair synthesis in primary human fibroblasts by incorporation of ethynyl deoxyuridine (EdU)

Siripan Limsirichaikul[1,2], Atsuko Niimi[1,3], Heather Fawcett[3], Alan Lehmann[3], Shunichi Yamashita[1] and Tomoo Ogi[1,*]

[1]Department of Molecular Medicine, Atomic Bomb Disease Institute, Nagasaki University, Nagasaki, 852-8523 Japan, [2]Department of Biopharmacy, Faculty of Pharmacy, Silpakorn University, Nakhon Pathom, 73000 Thailand and [3]Genome Damage and Stability Centre, University of Sussex, Falmer, Brighton, BN1 9RQ, UK

Received September 25, 2008; Revised and Accepted January 7, 2009

ABSTRACT

Xeroderma pigmentosum (XP) is an autosomal recessive genetic disorder. Afflicted patients show extreme sun-sensitivity and skin cancer predisposition. XP is in most cases associated with deficient nucleotide excision repair (NER), which is the process responsible for removing photolesions from DNA. Measuring NER activity by nucleotide incorporation into repair patches, termed 'unscheduled DNA synthesis (UDS)', is one of the most commonly used assays for XP-diagnosis and NER research. We have established a rapid and accurate procedure for measuring UDS by replacement of thymidine with 5-ethynyl-2'-deoxyuridine (EdU). EdU incorporated into repair patches can be directly conjugated to fluorescent azide derivatives, thereby obviating the need for either radiolabeled thymidine or denaturation and antibody detection of incorporated bromodeoxyuridine (BrdU). We demonstrate that the EdU incorporation assay is compatible with conventional techniques such as immunofluorescent staining and labeling of cells with micro-latex beads. Importantly, we can complete the entire UDS assay within half a day from preparation of the assay coverslips; this technique may prove useful as a method for XP diagnosis.

INTRODUCTION

Cells are continuously exposed to various types of DNA damage induced by both endogenous and exogenous sources. Consequently, all living organisms have developed DNA repair mechanisms to ensure that the integrity of the genetic information is maintained (1). Nucleotide excision repair (NER) is one of the most versatile DNA repair systems, which deals with the major UV photoproducts, as well as many DNA adducts arising from exposure to a variety of chemical carcinogens (2,3). NER involves removal of damaged nucleotides from the DNA by dual incisions, and filling and sealing of the residual single-strand gaps by DNA polymerases and ligases (1–3).

Xeroderma pigmentosum (XP) is the prototype NER-deficient genetic disorder (2–4), the incidence of which is 1 in 80 000 to 1 000 000 in the general population, depending on the location (5). XP patients suffer from severe photosensitivity, a high incidence of sunlight-induced skin cancer and in some cases neurological abnormalities. In ~80% of XP cases, the patients have a defect in one of the genes responsible for NER. XP-variant patients, who comprise the residual 20% of XP cases, are proficient in NER but have a defect in post-replication repair (PRR) as they lack the specialized DNA polymerase, polη, which accurately replicates past cyclobutane pyrimidine dimers (CPDs) (6).

Cockayne syndrome (CS) and Trichothiodystrophy (TTD) are also NER-deficient disorders (4,7,8). NER consists of two sub-pathways: global genome repair (GGR) is relatively slow but functions genome wide (3), whereas transcription-coupled repair (TCR) is a faster process that is specialized for the transcribed strand of actively transcribed regions (9,10). With the exception of XPC and XPE, which are used exclusively in GGR (3), all genes defective in patients with XP, the combined features of XP and CS (XP/CS), and TTD are associated with both pathways, whereas in CS only TCR is compromised (7,9–11). NER-deficient patients have been so far assigned to at least 11 complementation groups (XP-A to G, CS-A and B, TTD-A and ERCC1), which correspond

*To whom correspondence should be addressed. Tel: +81 95 819 7103; Fax: +81 95 819 7104; Email: togi@nagasaki-u.ac.jp

The authors wish it to be known that, in their opinion, the fourth and the fifth author contributed equally to the work.

to 11 different NER damage recognition and incision proteins (3,4).

The most commonly used assay for assessing NER-deficiency entails measuring nucleotide incorporation levels associated with DNA-repair activity. GGR, which contributes to ~90% of NER activity, is assessed by damage induced non-S-phase gap-filling DNA replication, termed 'unscheduled DNA synthesis (UDS)' (12), while TCR activity can be measured by 'recovery of RNA synthesis (RRS)' levels after DNA-damaging treatment (13). Currently, a variety of methods for measuring UDS have been established (8,12,14–17). For inducing DNA damage 254-nm UVC-irradiation is commonly used and cells are then incubated in the presence of either radiolabeled thymidine or a nucleoside analog. The most frequently used methods in XP-diagnostic laboratories are: (i) ^{3}H-thymidine incorporation, followed by evaluation of grain counting after autoradiography of tissue-culture coverslips—this technique is accurate and compatible with most immunostaining-based methods, but the procedures are labor-intensive and time-consuming (15,16). (ii) Bromodeoxyuridine (BrdU) incorporation, followed by alkaline denaturation of DNA, and immunofluorescent detection by anti-BrdU antibody—this is a convenient variant of method (i); replacement of ^{3}H-thymidine by BrdU diminishes the time needed for the assay, however it has reduced sensitivity (~50% reduction of UDS activity is not detectable) (18). (iii) Liquid scintillation counting of ^{3}H-thymidine incorporation into repair patches—although this method is rapid, the quantitative capacity is lower than the other methods as this is a batch assay. Furthermore, replicative DNA synthesis has to be abolished by using non-dividing cells and the DNA replication inhibitor, hydroxyurea (HU), during the assay (12).

In this report, we have employed 5-ethynyl-2′-deoxyuridine (EdU), an alkyne-conjugated nucleoside analogue of thymidine, as an alternative to radioactive thymidine or BrdU (19). In contrast to the BrdU-based UDS assay, EdU can be directly conjugated to fluorescent azide (20), and thus, the assay does not require denaturing of DNA nor the use of antibodies. We have successfully improved the sensitivity, which is one of the weak points of BrdU-based methods. Furthermore, the total time for the assay was dramatically reduced even compared to the BrdU-based assay. Using this technique, a standard UDS assay can be completed within half a day from preparation of the assay coverslips.

MATERIALS AND METHODS

Cell strains and cultures

All the cells used in this report are human primary fibroblasts. Normal 1BR (21), 48BR (21), 142BR (22) and 251BR (22), XP-patient-derived XP12BR (XP-D) (this study), XP15BR (XP-A) (22), XP13BR (XP-C) (this study) and XP20BE (XP-G) (23) and CS-patient-derived CS10LO (CS-B) (24) cells were used. Cells were cultured in Dulbecco's Modified Eagle Medium (DMEM) supplemented with 10% FBS (Gibco-BRL) and penicillin–streptomycin (Wako), and maintained at semi-confluent density during the experiments unless otherwise stated. For labeling with latex-beads, 48BR cells were cultured with a few drops of 0.5-μm diameter polybead Hydroxylate (Polysciences) in DMEM for 3 days.

UV-induced UDS measurement in normal primary human fibroblasts by EdU incorporation

5-ethynyl-2′-deoxyuridine (EdU) is available from *Invitrogen* (19). To optimize UV-induced UDS by EdU incorporation, effects of UV dose and EdU-incubation period were examined. 48BR cells were cultured on coverslips and maintained at confluent density. Cells were washed with PBS, followed by irradiation with different doses (5–20 J/m^2) of UVC (254 nm). After UV irradiation, cells were immediately incubated with serum-free DMEM supplemented with 10 μM EdU for different periods (0.5, 1, 2 and 4 h). Serum-free medium was used since serum often contains thymidine, which competes with EdU for incorporation into DNA. Cells were then washed with PBS, followed by fixation and permeabilization with PBS containing 2% formaldehyde, 0.5% triton X-100 and 300 mM sucrose for 20 min. After extensive washing with PBS, cells were blocked with 10% FBS in PBS for 30 min. Incorporated EdU was detected by fluorescent-azide coupling reaction (Click-iT, *Invitrogen*) (19). Briefly, cells were incubated for 30 min with azide-conjugated Alexa Fluor 488 dye in TBS supplemented with 4 mM $CuSO_4$. Cells were then washed three times with PBS containing 0.05% Tween-20 (PBST). Coverslips were finally soaked with PBS, fixed with 3.7% formaldehyde in PBS for 20 min, and mounted on glass slides with Aquapolymount (Polysciences). Photographs of the cells were captured with a fluorescent microscope equipped with a CCD camera (BIOREVO9000-KEYENCE), and captured images were processed and analysed with ImageJ software (NIH). At least 50 non-S-phase cells were randomly selected from a single captured field, and the average nuclear fluorescent intensity was calculated. Data points presented in the text are the averages calculated from five different fields.

We found that 20 J/m^2 UV irradiation followed by 2-h EdU incubation was the optimal condition for the UDS assay. This condition was used for all experiments except for Figures 1A and 5.

BrdU incorporation assay

Cells were cultured and UVC irradiated (20 J/m^2), and incubated in conditions identical to the EdU-incorporation assay described above (5 μM BrdU, instead of EdU, was supplemented). Cells were then washed with PBS, followed by fixation and permeabilization in PBS containing 2% formaldehyde, 0.5% tritonX-100 and 300 mM sucrose for 20 min. After extensive washing with PBS, cells were treated with 4 M HCl in PBS for 15 min for denaturing DNA. Cells were extensively washed with PBS for neutralization, followed by blocking with 10% FBS in PBS for 30 min. Incorporated BrdU was detected by 1-h incubation with mouse anti-BrdU antibody (BD, diluted 1:150 in PBST). Cells were then washed three times with

PBST, followed by 1-h incubation with Alexa Fluor 488-conjugated goat anti-mouse IgG (*Invitrogen*, diluted 1:500 in PBST). Coverslips were finally soaked in PBS, fixed with 3.7% formaldehyde in PBS for 20 min, and mounted on glass slides with Aquapolymount (Polysciences). Image capture and analyses were performed as described above.

^{3}H-thymidine incorporation assay

Details of the assay have been previously described (12). Cells were cultured in 1% DMEM for 3 days (3×10^5 cells per 5-cm-diameter dish). They were then incubated for 1 h with 10 mM hydroxyurea (HU), UV irradiated and incubated for a further 3 h with 1% DMEM containing 10 μCi/ml ^{3}H-thymidine and 10 mM HU. ^{3}H-thymidine incorporated into acid-insoluble materials was measured by liquid scintillation counting.

Immunostaining

48BR and XP20BE cells were mix-cultured at 1:1 ratio (48BR alone for ki67 staining). UV irradiation, EdU incubation and fixing and permeabilization steps were as described above. For antibody detection, cells were blocked with 10% FBS in PBS for 30 min, followed by 1-h incubation with mouse monoclonal anti-XPG (8H7, Santa Cruz Biotechnology), or rabbit monoclonal anti-ki67 (SP6, Thermo scientific) antibodies (diluted 1:100 in PBST). Cells were then washed three times with PBST, followed by 1-h incubation with secondary antibodies: Alexa Fluor 594-conjugated goat-anti-mouse-, and goat-anti-rabbit-IgG, for XPG and ki67 detection, respectively (Invitrogen, diluted 1:1000 in PBST). To avoid unnecessary nuclear fluorescence, DAPI staining was omitted. After extensive washing with PBST, cells were fixed for 20 min with 3.7% formaldehyde in PBS. Subsequently, EdU detection was carried out as described above.

RESULTS

Effects of UV dose and EdU-incubation period on measurement of UV-induced UDS in normal human primary fibroblasts

48BR normal primary human fibroblasts were cultured on coverslips and subsequently exposed to different doses of UVC, followed by incorporation of EdU for different time periods. UVC treatment elicited UDS activity as shown by an increase in nuclear fluorescence, after conjugation of fluorescent azide to incorporated EdU (Figure 1A and B). As reported in previous publications employing ^{3}H-thymidine labeling and autoradiography (15,16), strong signals from scheduled DNA synthesis in S-phase cells can be distinguished from much weaker cell-cycle independent unscheduled EdU incorporation, resulting from repair synthesis (Figure 1B). Additionally, the fluorescent-azide coupling reaction seems specific to incorporated EdU, as we barely detected any non-specific cytoplasmic staining or DNA-replication-independent nuclear signals (Figure 1B). We observed that the nuclear fluorescent intensities were proportional to both UV dose and EdU-incubation time, indicating that this end-point satisfactorily represents the amount of incorporated EdU, which is directly convertible to semi-quantitative UDS measurement (Figure 1A). We were able to detect nuclear fluorescent signals at relatively low UV exposures, and with short time-periods of post-UV EdU incubation, demonstrating that this technique is sensitive enough to detect low levels of UDS activity.

Sensitivity and resolution of the EdU-based UDS assay

We evaluated the resolution as well as the sensitivity of the EdU-based UDS assay, by comparing the results obtained from the EdU technique with that of conventional autoradiography and BrdU-based methods. Many publications that have utilized autoradiography for the UDS assay report UDS levels for the most severe XP cases (i.e. XP-A or XP-G/CS) as <5–10% of normal levels (25). These can be distinguished from cell strains from XP patients, typically from XP-C or XP-D groups, which often have UDS levels of 20–40% of residual UDS activity (intermediate UDS level). The intensity-distribution plots for the EdU-based UDS assay for both normal 48BR (UDS positive, Figure 1C) and XP-deficient XP15BR (UDS negative, Figure 1D) fibroblasts resemble those of published autoradiography-based experiments, though we acknowledge that the background UDS levels were relatively higher than that from autoradiography (this point is discussed later). The EdU assay consistently produced a satisfactory SD of 10–15%.

We compared the relative sensitivities of the EdU assay and the BrdU-based method. Though BrdU has been commonly used for S-phase labeling, publications using it for UDS assays are quite limited because of its restricted sensitivity and resolution (18) (Figure 1E and F). Although the histograms of normal 48BR and XP-deficient XP15BR fibroblasts could be discriminated by the BrdU-based assay (Figure 1E and F), the resolution as well as SD were both markedly improved in the EdU method, suggesting that EdU is a more sensitive substitute for BrdU in the UDS assay.

UV-induced EdU incorporation in NER-deficient primary fibroblasts

To apply the EdU technique to XP diagnosis, we estimated the levels of UV-induced EdU incorporation in several NER-deficient primary fibroblasts as well as normal controls (Figure 2A–G for histograms, and Figure 2I for typical photos). Since XP is a genetically heterogenous disorder, both the NER genes affected and the types of mutations determine the magnitude of the defect in UDS. We measured UDS in XP15BR (XP-A), XP20BE (XP-G/CS), XP13BR (XP-C), XP12BR (XP-D) and CS-patient-derived CS10LO (CS-B) cells, and compared the results with those obtained using ^{3}H-thymidine incorporation. With 20 J/m^2 UVC irradiation, we observed substantial UDS in normal fibroblasts, 48BR (Figure 2A) and 1BR (Figure 2B), as measured by EdU incorporation. We barely detected any UDS in severe XP-patient-derived XP15BR (XP-A, Figure 2C) and XP20BE (XP-G, Figure 2D) fibroblasts, while we detected

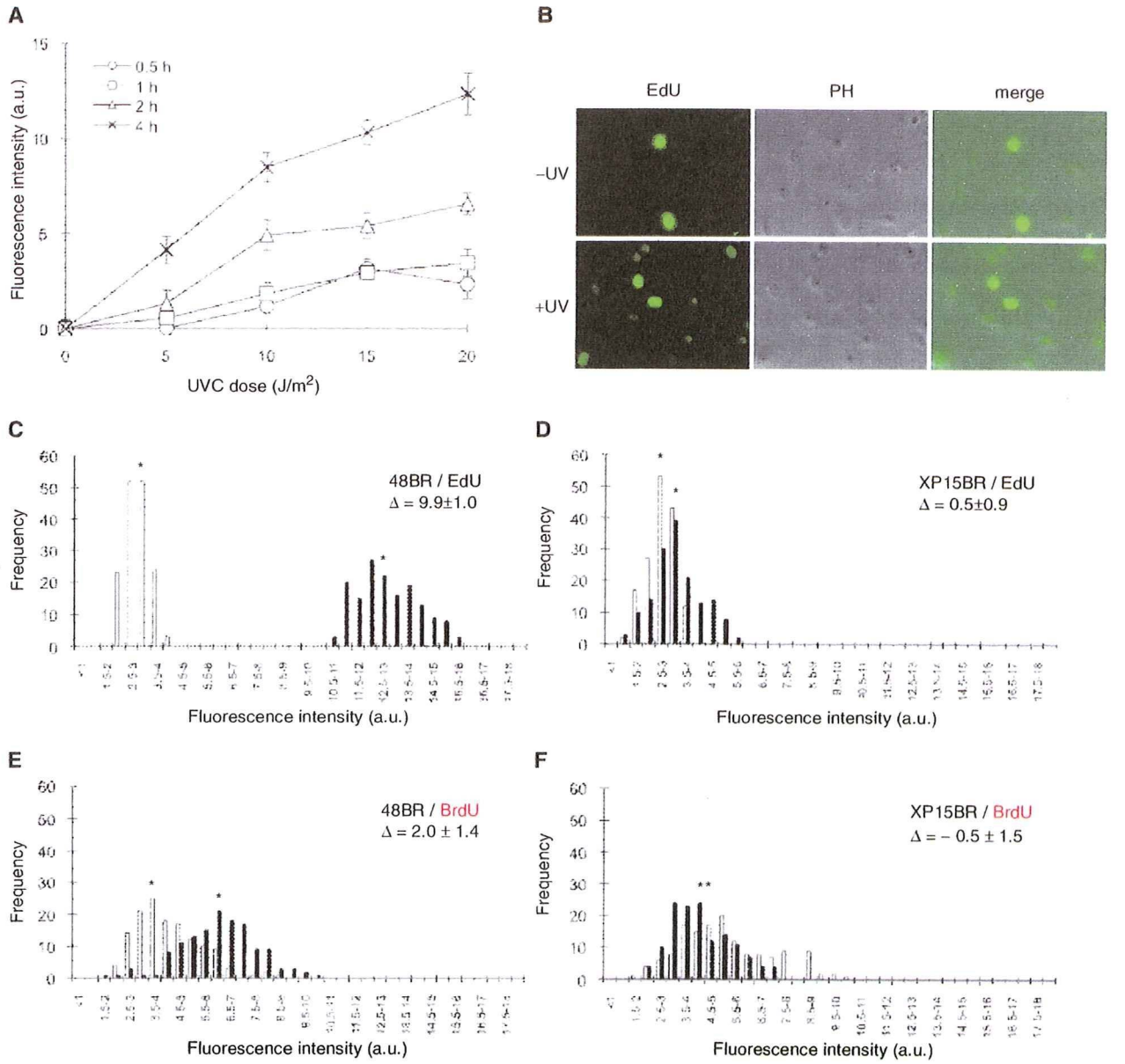

Figure 1. UV-induced UDS assay in normal human primary fibroblasts. (**A**) Normal 48BR cells were cultured on coverslips, UVC-irradiated at the indicated doses, followed by incubation with 10 μM EdU for different time periods, fixation and conjugation of fluorescent dye to the incorporated EdU as described in 'Materials and methods' section. The intensity of nuclear fluorescence, which is associated with UDS activity, was analysed using a fluorescence microscope and image-processing software. For each data point, at least 250 nuclei were analysed. Points and error bars indicate means of discrete nuclei fluorescent intensity and standard errors, respectively. (**B**) Typical photos of the EdU assay are shown. 48BR cells were UVC irradiated (20 J/m^2, +UV) or mock-treated (−UV), followed by 2-h incubation with EdU. EdU, coupled to Alexa fluor 488-azide; PH, phase contrast. (**C–F**) UDS performed by incorporation of EdU (C and D) or BrdU (E and F) was compared. XP15BR cells are primary fibroblasts from an XP-A patient. Cells were UVC irradiated (20 J/m^2), followed by incubation with 10 μM EdU or 5 μM BrdU for 2 h. Bars represent frequencies of the fluorescence levels in the indicated classes, with (black) or without (white) UVC irradiation. Asterisks indicate the mean values of nuclear fluorescent intensities, which correspond to the UDS levels. Δ represents UDS difference between irradiated and unirradiated samples.

marginal (~20% of normal) UDS activity in XP-C patient-derived XP13BR (Figure 2E) fibroblasts.

XP12BR is homozygous for R511Q mutation in the *XPD* gene (our unpublished data), and, as shown in Figure 2F, we found ~40% of normal UDS activity. In Figure 2H, we show the data obtained with the same set of cell strains using the ^{3}H-thymidine incorporation. In good agreement with the EdU assay, UDS was barely detectable in XP15BR, but were about ~20% and ~40% of normal in XP13BR and XP12BR, respectively. These results show good agreement between the two methods and demonstrate that cells exhibiting intermediate UDS activity

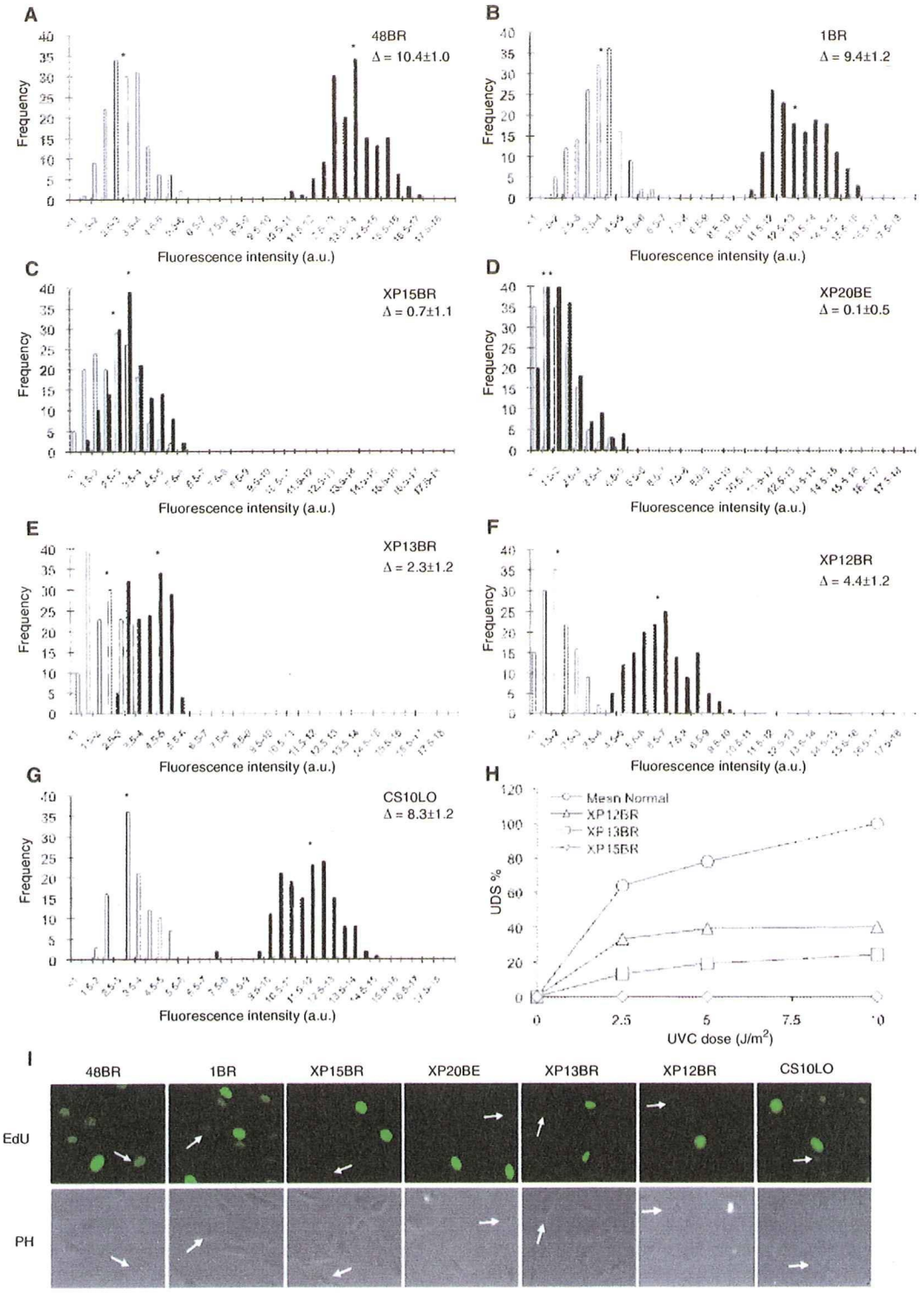

Figure 2. UV-induced EdU incorporation in non-S-phase cells is NER repair replication specific. (**A–G**) Levels of UV-UDS in NER-proficient and NER-deficient cells were examined. Primary fibroblasts were cultured on coverslips, UVC-irradiated (20 J/m^2), followed by 2-h incubation with 10 μM EdU. Levels of EdU incorporation were analysed as in Figure 1A and presented as in Figure 1. (**H**) UDS assay performed by ^{3}H-thymidine incorporation. Quiescent cells were UVC irradiated at the indicated dose and ^{3}H-thymidine incorporation was measured for 3 h after UVC irradiation in the media containing 10 mM hydroxyurea. UDS levels were normalized and expressed as percentages of the UDS in the normal cells at 10 J/m^2. Mean Normal represents the average UDS levels of the four different normal cell lines (1BR, 48BR, 142BR and 251BR). Asterisks indicate the mean values of nuclear fluorescent intensities, which correspond to the UDS levels. Δ represents UDS difference between irradiated and un-irradiated samples. (**I**) Typical photos of the EdU incorporation examined in Figure 2A–G are shown (2 h after 20 J/m^2 UVC irradiation). Arrows indicate non-S-phase cells. 48BR, normal; 1BR, normal; XP15BR, XP-A; XP20BE, XP-G; XP13BR, XP-C; XP12BR, XP-D; CS10LO, CS-B.

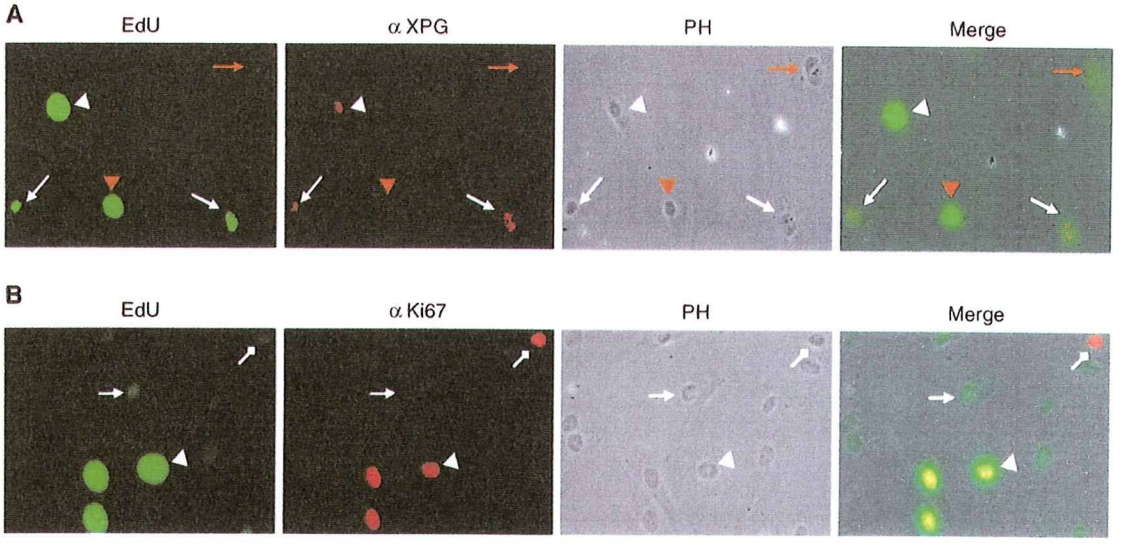

Figure 3. EdU assay is compatible with immunostaining. (**A**) Normal 48BR and XPG-deficient XP20BE fibroblasts were co-cultured on coverslips, UVC irradiated (20 J/m^2), followed by 2-h incubation with 10 μM EdU. Fixed cells were then immunostained with rabbit anti-XPG antibody (red), followed by conjugation of Alexa fluor 488-azide to incorporated EdU (green). (**B**) UV-induced EdU incorporation in quiescent cells. 48BR cells were UVC irradiated (20 J/m^2), followed by 2-h incubation with 10 μM EdU. Fixed cells were then immunostained with rabbit anti-ki67 antibody (red), followed by conjugation of Alexa fluor 488-azide to incorporated EdU (green). Triangle, normal arrow and diamond arrow indicate S-phase, G0 and G1 (or G2/M), respectively. Detailed experimental conditions are described in 'Materials and methods' section.

can be distinguished from both normal and severe UDS defects by the EdU-based assay.

We then further examined whether CS-deficient fibroblasts were distinguishable from normal cell lines by the UDS assay. CS is only compromised in the TCR pathway of NER, and this is not precisely diagnosed by UDS assays, since the deficiency is usually subtle. Though Figure 2G indicates a modest (~20%) reduction of the UDS level compared to the normal fibroblasts, we cannot conclude this to be significant and is likely to fall within the normal range.

Levels of nuclear fluorescence after UVC irradiation in severe NER-deficient fibroblasts (Figure 2C and D) were virtually the same as those in unirradiated samples, suggesting that the background fluorescent signals resulting from minor EdU incorporation or non-specific fluorescent conjugation do not affect the analyses. We conclude that the EdU-based UDS assay provides a specific measurement of nucleotide incorporation associated with the repair synthesis step of NER.

Compatibilities of the EdU-based UDS assay with other techniques

We anticipate applying the EdU-based UDS assay system to clinical diagnoses, in which rigorous intra-assay controls are required. We therefore assessed the compatibility of the UDS assay with other standard techniques that use internal references. We found that fluorescent-azide conjugation to EdU is fully compatible with immunofluorescent staining (Figure 3A and B).

Co-culture of an index fibroblast as well as a target under study on the same coverslip provides a rigorous internal control. In Figure 3A, normal and XPG-deficient fibroblasts were co-cultured, followed by UV-UDS assayed in combination with α-XPG immunostaining. EdU-positive cells (excluding S-phase) perfectly correspond to XPG-positive cells, indicating that two different cell populations can be distinguished in the UDS assay.

Similarly, we examined if there was a cell-cycle preference for the EdU assay: co-immunostaining with a proliferation marker, ki-67, demonstrated that UDS can be detected in quiescent fibroblasts (no Ki67 stain) as well as proliferating populations (Figure 3B).

As discussed above, the level of the defect in UDS activity varies between different XP patients. Ideally, ascertaining whether a patient is NER compromised is evaluated by comparing the residual UDS activity of the patient-derived fibroblast with index cells. For this purpose, in a practical UDS-based XP diagnosis, normal fibroblasts have been preloaded with latex-beads in the cytoplasm and co-cultured with patient-derived fibroblasts. The 'bead-labeled-cells' provide an internal standard that can be detected under phase contrast microscopy which eliminates sample-to-sample staining variability (15). We tested if this technique is also compatible with the EdU assay. First we checked whether the latex-beads did not affect the nuclear fluorescent intensity. As shown in Figure 4A (top panel) and corresponding histogram (Figure 4B), the fluorescent intensity in 48BR cells loaded with beads was practically the same as those in cells without beads, indicating that the beads do not interfere with the EdU-based UDS assay.

Modest (XP12BR; Figure 4A middle panel and 4C) as well as severe (XP15BR; Figure 4A bottom panel and 4D) UDS-deficient fibroblasts were both easily distinguishable from co-cultured 48BR fibroblasts by their nuclear

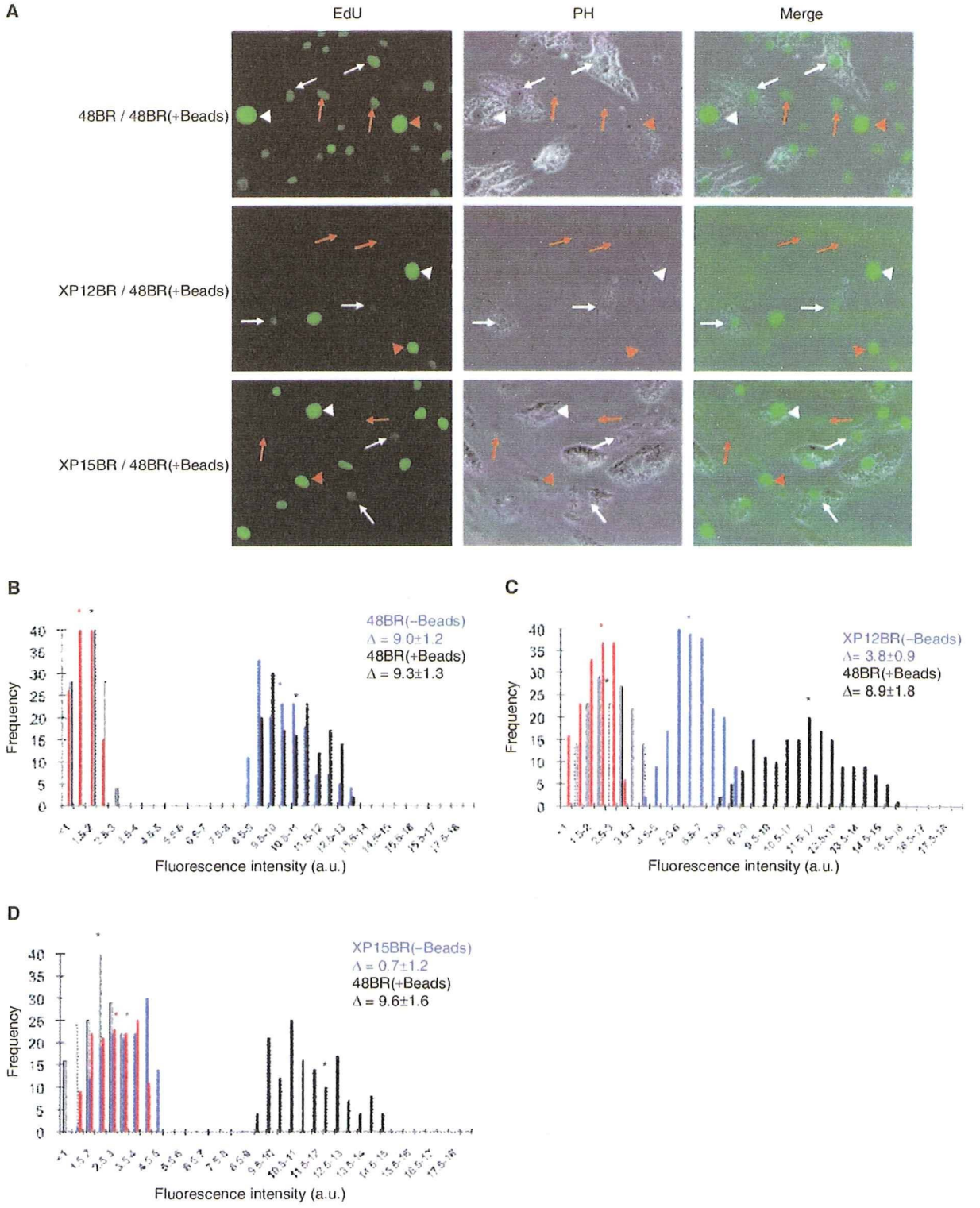

Figure 4. EdU assay in the presence of latex beads. Normal 48BR cells were pre-labeled with 0.5-μm diameter latex beads and co-cultured with indicated XP fibroblasts (no-beads) on coverslips. Cells were then UVC-irradiated (20 J/m^2), followed by 2-h incubation with 10 μM EdU. Coverslips were then processed as in Figure 1. (**A**) Typical photos are displayed. White and red markings, arrows and arrow heads represent 48BR and indicated XP cells, and non-S-phase and S-phase cells, respectively. (**B–D**) Histograms of the UDS assay with the internal standard 48BR and (B) 48BR, normal; (C) XP12BR, XP-D; and (**D**) XP15BR, XP-A. Bars represent frequencies as described in Figure 1, with (black, 48BR; blue, XP cell-lines) or without (white, 48BR; red, XP cell-lines) UVC irradiation. Asterisks indicate the mean values of nuclear fluorescent intensities, which correspond the UDS levels. Δ represents UDS differences with or without UVC irradiation.

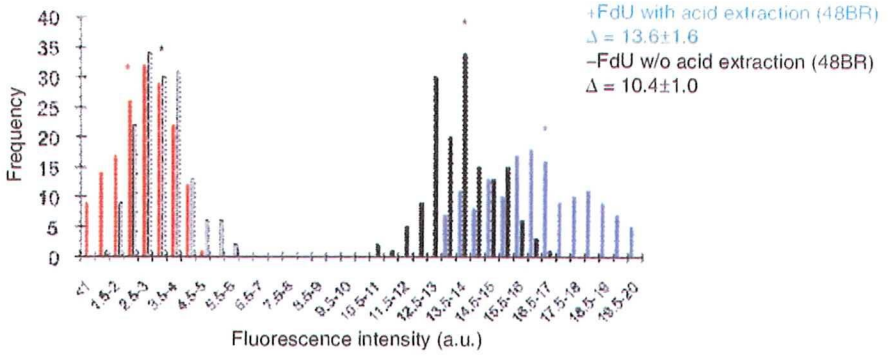

Figure 5. Improvement of the sensitivity by FdU supplement, longer incubation and acid extraction. Normal 48BR cells were cultured on coverslips, UVC irradiated (20 J/m^2), followed by incubation with 10 μM EdU and 1 μM FdU (Sigma) for 4 h. Cells were then fixed as indicated in Figure 2. Acid extraction was performed using Bouin's fixative (Sigma) for 30 min, followed by extensive washing with PBS. Conjugation of fluorescent dye and detection of EdU signals were identical to the experiments in Figure 2. Bars represent frequencies of the fluorescence levels in indicated classes, with (black, identical to Figure 2A; blue, + FdU + 4-h incubation + acid extraction) or without (white, identical to Figure 2A; red, + FdU + 4-h incubation + acid extraction) UVC irradiation. Asterisks indicate the mean values of nuclear fluorescent intensities. Δ represents UDS differences with or without UVC irradiation.

fluorescent levels. The UDS measurements with or without internal controls were nearly the same (compare Figure 2A, 2C and 2F with Figure 4B, 4D and 4C), suggesting that the prep-to-prep or coverslip-to-coverslip variation in the EdU-based assay is small; this may be an advantage when applying the EdU assay to experiments that are incompatible with the use of an internal standard (e.g. fluorescent-based high-throughput screening using GE's In-Cell-Analyzer or flow cytometry).

Further optimization of the EdU assay

The EdU-based experiments described above are sufficient for routine XP screening as well as many types of NER research; however, further precise experiments such as distinguishing between no UDS activity and very low levels may require higher sensitivity. We have attempted to increase the specific EdU uptake as well as to reduce the non-specific background. The incorporation of a thymidine analogue into the DNA is dependent on its concentration relative to endogenously synthesized thymine nucleotides in the nucleotide pool. Fluorodeoxyuridine (FdU) is an inhibitor of thymidylate synthetase, which renders the cell dependent on exogenously supplied thymidine or its analogues. We therefore used FdU and a longer incubation period (4 h) after UV irradiation. Additionally, we used stringent acid extraction with Bouin's fixative to try and reduce the background. As shown in Figure 5, although not dramatic, both background (compare white and red bars and their corresponding asterisks) and UDS-specific EdU uptake (compare black and blue bars) were improved.

DISCUSSION

Rapid and accurate assessment of UDS levels is indispensable for clinical XP diagnosis as well as NER research. In this report, we have described a novel UDS assay system that provides a very simple method for measurement of repair-replication activity in human cells.

Orthodox UDS assay methods have been based on ^{3}H-thymidine incorporation (12,15,16). Although a variety of alternative reagents have been developed, most XP-diagnosis laboratories still measure UDS by autoradiography or direct scintillation counting of incorporated ^{3}H-thymidine. The biggest disadvantages of using ^{3}H-thymidine for UDS assay is its time-consuming procedures and the requirement for laboratories designated for radioactive work.

The autoradiographic process provides an accurate measurement of UDS activity as each silver grain represents an individual event of nucleotide incorporation into a repair patch. However, the experiment is complicated, requiring significant skills, and takes 1–2 weeks to be completed; furthermore, counting of silver grains under the microscope is laborious. An alternative procedure uses direct scintillation counting of ^{3}H-thymidine incorporation (12). This method requires abrogation of S-phase DNA replication. To accomplish this, cells are brought into quiescence by serum starvation, and hydroxyurea is needed during the nucleotide incorporation period, to block replicative DNA synthesis. This technique significantly reduced the time required for the UDS assay, but quantitation of UDS is less accurate.

In contrast to the above ^{3}H-thymidine-based methods, BrdU incorporation assay is faster and a convenient option. Indeed, BrdU has been frequently used for cell-cycle analysis applications. On the other hand, regardless of the type of experiments, denaturation of DNA is needed to detect the incorporated BrdU as the anti-BrdU antibody is too big to access the epitope in native DNA. DNA denaturation and subsequent immunofluorescence detection sometimes generate an ambiguous staining pattern (data not shown; see high SD in Figure 1E and F). This is the biggest disadvantage of the BrdU incorporation assay: nucleotide incorporation into repair patches based on DNA-repair activity is quite low and difficult to detect. For this reason, UDS based on BrdU has not been widely used.